

Kent Academic Repository

Full text document (pdf)

Citation for published version

Georgiou, Leoni and Kivell, Tracy L. and Pahr, Dieter H. and Buck, Laura T. and Skinner, Matthew M. (2019) Trabecular architecture of the great ape and human femoral head. *Journal of Anatomy* . ISSN 0021-8782. (In press)

DOI

<https://doi.org/10.1111/joa.12957>

Link to record in KAR

<https://kar.kent.ac.uk/72752/>

Document Version

Author's Accepted Manuscript

Copyright & reuse

Content in the Kent Academic Repository is made available for research purposes. Unless otherwise stated all content is protected by copyright and in the absence of an open licence (eg Creative Commons), permissions for further reuse of content should be sought from the publisher, author or other copyright holder.

Versions of research

The version in the Kent Academic Repository may differ from the final published version.

Users are advised to check <http://kar.kent.ac.uk> for the status of the paper. **Users should always cite the published version of record.**

Enquiries

For any further enquiries regarding the licence status of this document, please contact:

researchsupport@kent.ac.uk

If you believe this document infringes copyright then please contact the KAR admin team with the take-down information provided at <http://kar.kent.ac.uk/contact.html>

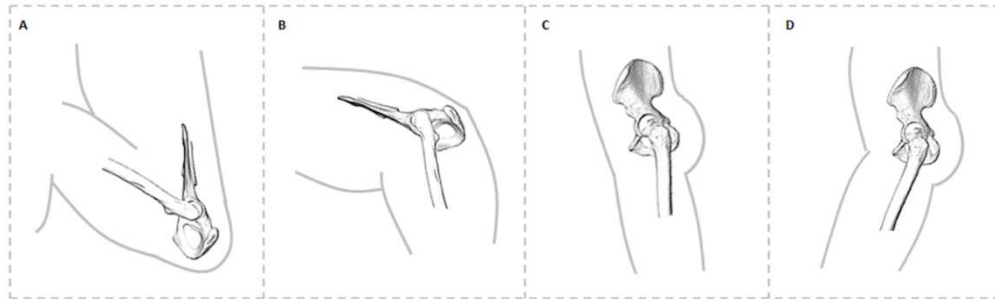


Figure 1. Comparison of hip posture during different habitual locomotor activities in great apes (A-B) and humans (C-D). (A) Great ape hip posture in maximum hip flexion (~ 55 - 60 degrees) during climbing (Isler, 2005). (B) Great ape hip posture at toe-off (~ 110 degrees) during terrestrial knuckle-walking (Finestone et al. 2018). (C) Human hip posture at toe-off (~ 175 degrees). (D) Human hip posture at heel-strike (~ 160 degrees).

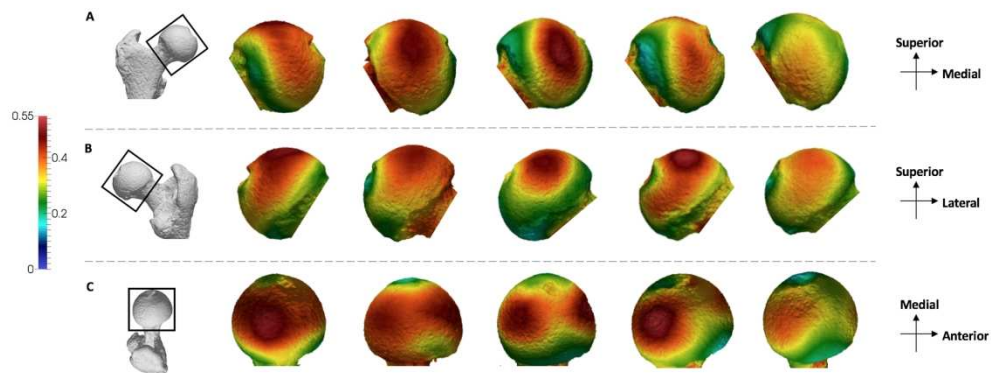


Figure 2. *Pan* BV/TV distribution in the femoral head. Five *Pan* specimens showing variation in the BV/TV distribution across the sample in (A) anterior, (B) posterior and (C) superior views. BV/TV is scaled to 0–0.55. All specimens are from the right side. Specimens from left to right (F-female, M-male): MPITC 14996 (F), USNM 220063 (F), USNM 176228 (M), MPITC 11781 (M), MPITC 11786 (F).

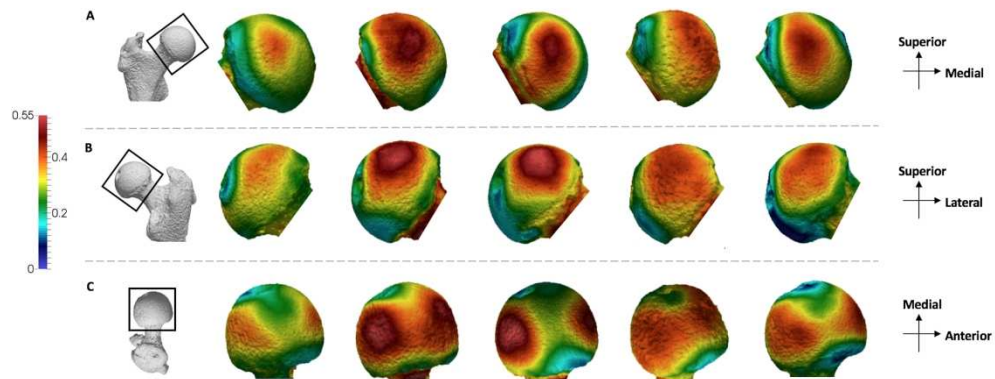


Figure 3. *Gorilla* BV/TV distribution in the femoral head. Five *Gorilla* specimens showing variation in the BV/TV distribution across the sample in (A) anterior, (B) posterior and (C) superior views. BV/TV is scaled to 0-0.55. All specimens are from the right side. Specimens from left to right (F-female, M-male): M96 (F), M264 (M), M372 (M), M856 (F), FC123 (M).

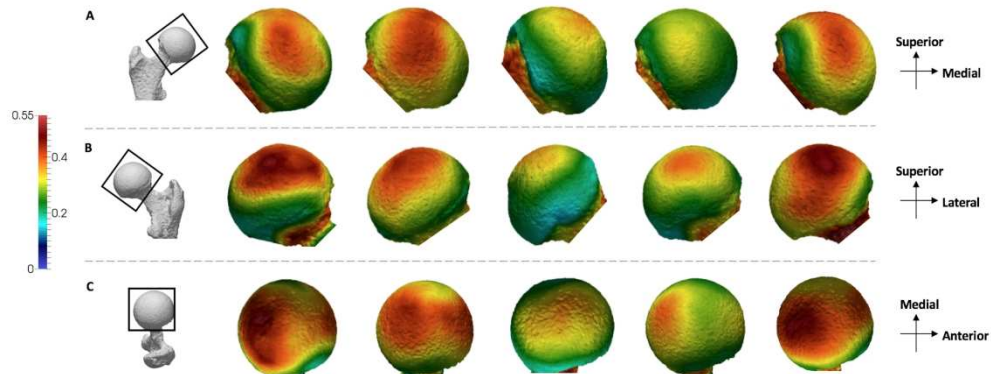


Figure 4. *Pongo* BVTV distribution in the femoral head. Five *Pongo* specimens showing variation in the BV/TV distribution across the sample in (A) anterior, (B) posterior and (C) superior views. BV/TV is scaled to 0-0.55. All specimens are from the right side. Specimens from left to right (All female): ZSM 1909 0801, 1907 0660, 1973 0270, 1907 0483, 1907 0633b.

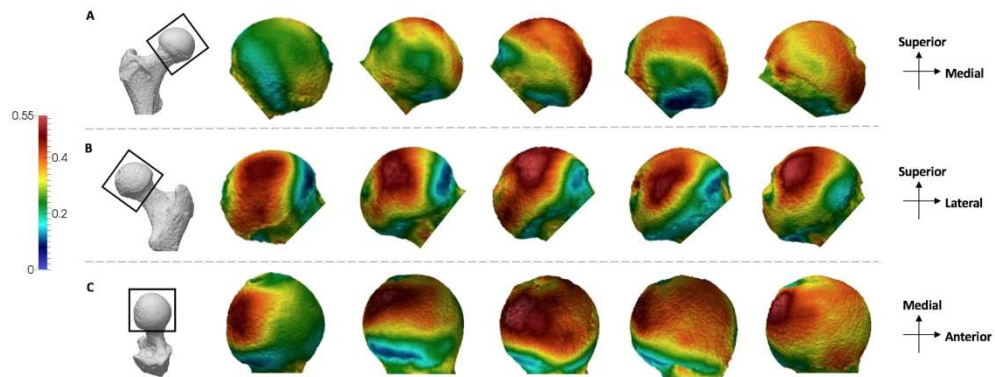


Figure 5. *Homo* BV/TV distribution in the femoral head. Five *Homo* specimens showing variation in the BV/TV distribution across the sample in (A) anterior, (B) posterior and (C) superior views. BV/TV is scaled to 0-0.55. All specimens are from the right side. Specimens from left to right (F-female, M-male): CAMPUS 36 (F), CAMPUS 93 (M), CAMPUS 74 (F), CAMPUS 417 (sex unknown), CAMPUS 81 (M).

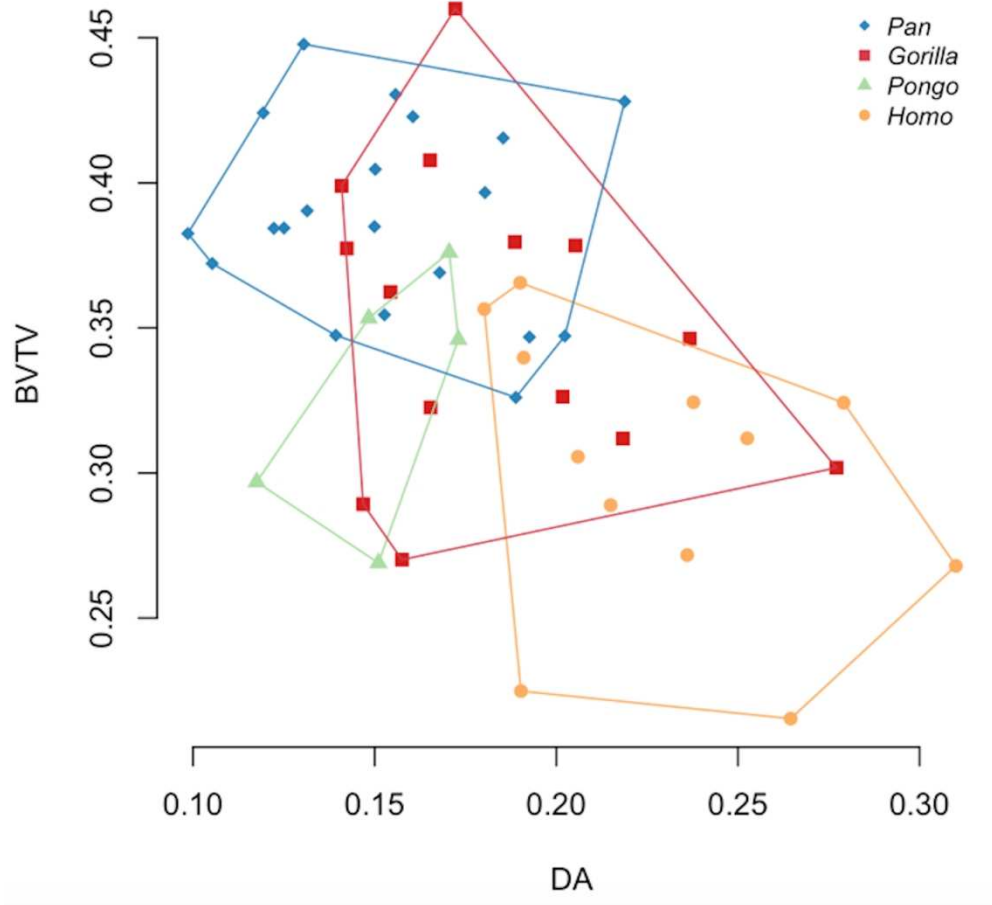


Figure 6. Bivariate plot of mean bone volume fraction (BV/TV) and mean degree of anisotropy (DA) for each individual and species in the sample.

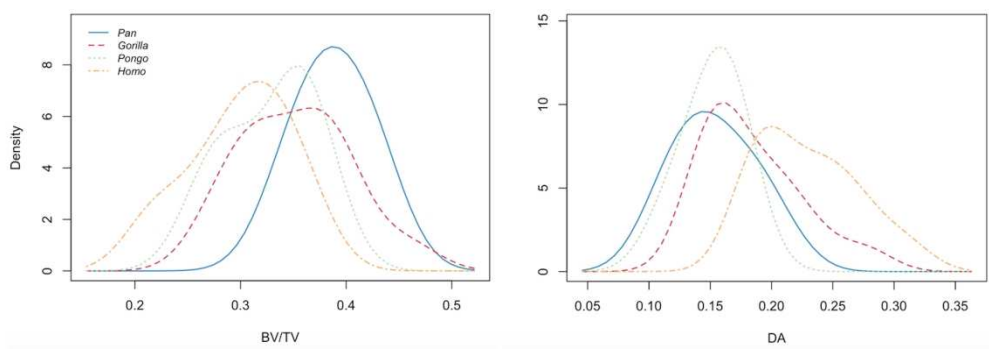


Figure 7. A histogram of mean BV/TV and DA value distributions in the studied taxa.

1 **Trabecular architecture of the great ape and human** 2 **femoral head**

3 Leoni Georgiou¹, Tracy L. Kivell^{1,2}, Dieter H. Pahr^{3,4}, **Laura T. Buck⁵**, Matthew M.
4 Skinner^{1,2}

5
6 ¹ Skeletal Biology Research Centre, School of Anthropology and Conservation,
7 University of Kent, Canterbury, United Kingdom

8
9 ² Department of Human Evolution, Max Planck Institute for Evolutionary
10 Anthropology, Leipzig, Germany

11
12 ³ Institute for Lightweight Design and Structural Biomechanics, Vienna University of
13 Technology, Vienna, Austria

14
15 ⁴ Department of Anatomy and Biomechanics, Karl Landsteiner Private University of
16 Health Sciences, Krems an der Donau, Austria

17
18 ⁵ **Department of Anthropology, University of California, Davis, California, United**
19 **States of America**

20
21
22 Corresponding Author:

23 Leoni Georgiou¹

24 School of Anthropology and Conservation, University of Kent, Canterbury, United
25 Kingdom

26 Email address: lg400@kent.ac.uk

27

28

29 **Trabecular architecture of the great ape and human femoral head**

30

31 **Abstract**

32

33 Studies of femoral trabecular structure have shown that the orientation and volume
34 of bone is associated with variation in loading and could be informative about
35 individual joint positioning during locomotion. In this study we analyse for the first
36 time trabecular bone patterns throughout the femoral head using a whole-epiphysis
37 approach to investigate how potential trabecular variation in humans and great apes
38 relates to differences in locomotor modes. Trabecular architecture was analysed
39 using microCT scans of *Pan troglodytes* (n=20), *Gorilla gorilla* (n=14), *Pongo* sp. (n=5)
40 and *Homo sapiens* (n=12) in medtool 4.1. Our results revealed differences in bone
41 volume fraction (BV/TV) distribution patterns, as well as overall trabecular parameters
42 of the femoral head between great apes and humans. *Pan* and *Gorilla* showed two
43 regions of high BV/TV in the femoral head, consistent with hip posture and loading
44 during **two discrete locomotor modes**; knuckle-walking and climbing. Most *Pongo*
45 specimens also displayed two regions of high BV/TV, but these regions were less
46 discrete and there was more variability across the sample. In contrast, *Homo* showed
47 only one main region of high BV/TV **in** the femoral head and had the lowest BV/TV,
48 **as well as the** most anisotropic trabeculae. The *Homo* trabecular structure **is**
49 **consistent with stereotypical loading with a more extended hip compared with great**
50 **apes, which is characteristic of modern human bipedalism**. Our results suggest that
51 holistic evaluations of femoral head **trabecular** architecture can **reveal previously**
52 **undetected patterns linked to** locomotor behaviour in extant apes and can provide
53 further insight into hip joint loading in fossil hominins and other primates.

54

55 **Key words:** hominid, African apes, *Gorilla*, *Pan*, *Pongo*, cancellous bone, functional
56 morphology.

57

58

59 **Introduction**

60

61 The morphology of the proximal femur has played a key role in the reconstruction of
62 locomotion in extant and extinct primates (e.g. McHenry and Corruccini, 1978; Burr et
63 al. 1982; Ruff et al. 1991; Ruff and Runestad, 1992; Ruff, 1995; Harmon, 2007;
64 Harmon, 2009a; Ruff and Higgins, 2013) and particularly **in understanding** the form
65 of bipedalism used by australopiths (Stern and Susman, 1983; Susman et al. 1984;
66 Crompton, et al. 1998; Carey and Crompton, 2005; Harmon, 2009b; Lovejoy and
67 McCollum, 2010; Raichlen et al. 2010; DeSilva et al. 2013). External morphology
68 provides **considerable** evidence of functional links between morphology and
69 locomotion. However, due to **possible** phylogenetic lag, **which results in traits that**
70 **are no longer functionally significant being present**, inferences about behaviour
71 based on external traits alone have been questioned (e.g. Ward, 2002). Variation in

72 internal trabecular bone structure across different regions of the skeleton can
73 provide additional evidence to help reconstruct joint postures and to infer potential
74 differences in locomotor behaviour in extant and extinct primates (e.g. Thomason
75 1985a,b; Ryan and Ketcham, 2002; Volpato et al. 2008; Ryan and Shaw, 2012; Tsegai
76 et al. 2013; Skinner et al. 2015; Stephens et al. 2016). Indeed, **the ability of trabecular**
77 **bone** to reflect mechanical loading was first **noted** in the human proximal femur
78 (Ward, 1838; Wolff 1870, 1892). It is not yet fully understood how mechanical or non-
79 mechanical factors trigger and ultimately affect the organisation of trabeculae. For
80 example, a range of activities, including **high strain/low frequency loading and low**
81 **strain/high frequency** loading have been shown to elicit trabecular reorganisation
82 (Rubin et al. 1990; Rubin et al. 2001; Judex et al. 2003; Wallace et al. 2014).
83 Furthermore, differences in body mass (Scherf, 2008; Cotter et al. 2009; Doube et al.
84 2011; Fajardo et al. 2013; Ryan and Shaw, 2013), hormones (e.g. Gunness-Hey and
85 Hock, 1984; Miyakoshi, 2004; Walsh, 2015), and genetic or systemic factors (Havill et
86 al. 2010; Tsegai et al. 2018) have been shown to influence aspects of trabecular
87 structure as well. However, computational (e.g. Huiskes et al. 2000; Keaveny et al.
88 2001) and experimental studies have demonstrated that modelling of trabeculae is
89 correlated with applied loads, and trabecular strut reorganisation can be instigated
90 by changes in the direction, magnitude and/or frequency of load (Biewener et al.
91 1996; Mittra et al. 2005; Pontzer et al. 2006; Polk et al, 2008; Barak et al. 2011).
92 Furthermore, trabecular bone volume fraction (BV/TV) and trabecular strut alignment
93 (degree of **anisotropy**, or DA) explain up to 98% of bone stiffness (i.e. Young's
94 modulus of elasticity) (Stauber et al. 2006; Maquer et al. 2015; Odgaard et al. 1997).
95 Thus, variation in the distribution of BV/TV and DA can provide insight into joint
96 loading and, in turn, locomotor behaviours in primates.

97
98 Several studies have revealed that variation in the trabecular architecture of the
99 primate hip and proximal femur is associated with differences in locomotion (e.g.
100 Rafferty and Ruff, 1994; MacLatchy and Muller, 2002; Volpato et al. 2008; Ryan and
101 Shaw, 2012; Saers et al. 2016). For example, Volpato and colleagues (2008)
102 demonstrated that the orientation of trabecular struts in the ilium and femoral neck
103 is associated with joint positioning in the hip of bipedally-trained Japanese macaques
104 and reflects alterations in the direction of load. **Comparable** changes in trabecular
105 structure **that reflect** differences in joint orientation were **also** found in the distal
106 femora of guinea fowls (Pontzer et al. 2006) and distal tibiae of sheep (Barak et al.
107 2011). **Furthermore, Scherf (2008) found that trabecular structure within the femoral**
108 **head, neck and both trochanters of climbing primates (e.g. *Alouatta seniculus*) had**
109 **more isotropic architecture, while specialised primates (e.g. *Homo sapiens*) in which**
110 **the femur experienced more stereotypical loading had more anisotropic structure.**
111 **Similar results were found in leaping primates, which in comparison to non-leaping**
112 **primate species, had more anisotropic trabeculae in the inferior aspect of the femoral**
113 **head (Ryan and Ketcham, 2002), and a different principal strut orientation (Ryan and**
114 **Ketcham, 2005).**

115
116 More recently, Ryan and Shaw (2012) investigated the trabecular patterns of the
117 femoral head in several anthropoid taxa and found that different suites of trabecular
118 variables could distinguish among taxa and locomotor groups. In particular, modern
119 humans were distinct in having relatively few, highly anisotropic trabeculae that are
120 thin and plate-like, *Pan* had relatively numerous, thick and isotropic trabeculae, while
121 *Pongo* had relatively few and isotropic trabeculae. Additional studies investigating
122 different human samples have also shown that femoral head trabecular structure
123 reflects variation in mobility levels, with more sedentary agriculturalists having
124 relatively low BV/TV compared with more active foragers (Ryan and Shaw, 2015;
125 Saers et al. 2016; Ryan et al. 2018). Interestingly, more active human foragers have
126 relatively high BV/TV that falls within the range of most extant hominoids apart from
127 *Pan* (Ryan et al. 2018). Despite this overlap in BV/TV between some human samples
128 and other hominoids, humans have consistently been shown to have the most
129 anisotropic femoral head structure compared to other great apes (Ryan and Shaw,
130 2015; Ryan et al. 2018). Furthermore, the human trabecular pattern has been shown
131 to develop during ontogeny when independent bipedalism develops and the gait
132 matures (Ryan and Krovitz, 2006; Reissis and Abel, 2012; Milovanovic et al. 2017).
133 Altogether, these studies suggest that the trabecular bone of the femoral head holds
134 a strong functional signal of locomotor loading in primates.

135
136 Conversely, other studies have failed to detect a strong locomotor signal in the
137 femoral head (Ryan and Walker, 2010; Shaw and Ryan, 2012), femoral neck (Fajardo
138 et al. 2007) and distal femur (Carlson et al. 2008). Carlson and colleagues (2008) did
139 not detect differences in the DA of the distal femoral metaphysis between mice with
140 turning locomotion and mice with non-turning locomotion. Similarly, Ryan and
141 Walker (2010) did not find any significant differences in the DA and BV/TV patterns
142 of the femoral head in a broad sample of platyrrhines and catarrhines. Furthermore,
143 Shaw and Ryan (2012), who examined the subarticular trabecular and mid-diaphyseal
144 cortical patterns in the femur and humerus of a sample of primates, concluded that
145 only the mid-diaphyseal cortical bone contains a clear functional signal linked to the
146 differential use of the two limbs between different locomotor groups.

147
148 The discrepancy in the findings of previous studies may, in part, be an artefact of the
149 volume-of-interest (VOI) method that was used. A VOI quantifies only a subsample of
150 trabecular structure within a given region and results can vary depending on its size
151 and position (Fajardo and Müller, 2001; Kivell et al. 2011). Additionally, challenges
152 arise when extracting homologous VOIs in taxa that vary in external morphology.
153 Prior research has demonstrated that additional functional insight can be gained
154 from investigating the trabecular architecture within an epiphysis as a whole (Tsegai
155 et al. 2013; Skinner et al. 2015; Stephens et al. 2016; Sylvester and Terhune, 2017;
156 Tsegai et al. 2018). Here we apply a whole-epiphysis approach to study the trabecular
157 structure throughout the femoral head of chimpanzees (*Pan troglodytes*), lowland

158 gorillas (*Gorilla gorilla*), orangutans (*Pongo* sp.) and humans (*Homo sapiens*), which
159 vary in locomotor behaviours and are relevant to the reconstruction of locomotion in
160 fossil hominins.

161

162 *Locomotion, hip morphology and predicted joint posture*

163

164 **Habitual locomotor activities and associated hip joint angles vary between great apes**
165 **and humans (Fig. 1).** Chimpanzees are predominantly terrestrial/arboreal
166 quadrupedal knuckle-walkers, but also engage frequently in arboreal climbing and,
167 less so, bipedalism (Hunt, 1991; Doran, 1992, 1993). **In all these locomotor modes,**
168 the hindlimb plays key role in propulsion and experiences higher vertical force than
169 the forelimb (Demes et al. 1994; Hannah et al. 2017). During terrestrial
170 quadrupedalism in chimpanzees, the mean hip angle at foot touchdown is 65° and at
171 toe-off it is 98.2° (Finestone et al. 2018). **Kinematics during chimpanzee vertical**
172 **climbing have, to our knowledge, only been studied in one individual and show that**
173 **the flexion-extension range at the hip increases substantially compared with**
174 **terrestrial quadrupedalism, with hip angles ranging from ~25° to ~105° (Nakano et**
175 **al. 2006). A more comprehensive study of bonobos (n=4 adults), which share similar**
176 **hindlimb anatomy with chimpanzees (e.g. Payne et al. 2006; Myatt et al. 2011),**
177 **yielded hip angles ranging from 55° to 135° during vertical climbing (Isler, 2005).**

178

179 Lowland gorillas are also predominantly quadrupedal knuckle-walkers (Remis, 1995;
180 Crompton et al. 2010). **They** often engage in arboreal climbing and bipedalism, **but**
181 **less frequently than chimpanzees** (Remis, 1995; Crompton et al. 2010). During
182 terrestrial quadrupedalism in gorillas, hip angles range from 77° at foot touchdown
183 to 120.6° at toe-off (Finestone et al. 2018). During vertical climbing, **hip angle range**
184 is similar to that of bonobos, ranging from approximately 45° to 135° (Isler, 2005).
185 *Gorilla* climbing frequency and technique varies with sex and body size, with the
186 range of hip flexion-extension being reduced in larger males compared to smaller
187 females (Remis, 1995; Remis, 1999; Isler, 2005). However, gorillas show less
188 intraspecific variation in climbing techniques than bonobos (Isler, 2005).

189

190 Orangutans employ a complex set of locomotor behaviours, which are mostly torso
191 orthograde, including vertical climbing, bridging, suspension from various limbs, and
192 terrestrial quadrupedalism (Cant, 1987; Isler and Thorpe, 2003; Thorpe and
193 Crompton, 2006; Thorpe et al. 2009). **Their hips are more mobile than those of other**
194 **apes**, which allows them to use their hindlimbs in more varied ways (Morbeck and
195 Zihlman, 1988; Tuttle and Cortright, 1988; Isler, 2005). During terrestrial locomotion,
196 the orangutan hip angle is 68.3° at touchdown and 107.3° at toe-off (Finestone et al.
197 2018). During vertical climbing, orangutans are able to lift their feet **further above**
198 **their hips than African apes**, such that their flexion-extension angle ranges from
199 around 30° to 135° (Isler, 2005).

200

201 Adult humans walk exclusively terrestrially on two legs, extending both their hips and
202 knees (Alexander, 1994). During the gait cycle, hip extension reaches 160° at
203 touchdown and 175° at toe-off (Abbass and Abdulrahman, 2014). Humans also
204 engage in running, which alters the joint angle of the hip and the resulting load on
205 the femoral head (Ounpuu, 1990; Ounpuu, 1994; van den Bogert et al. 1999;
206 Giarmatzis et al. 2015). Increase in speed is linked to more flexed hip joints and a
207 generally increased range of motion at the hip (Mann and Hagy, 1980; Novacheck,
208 1998). At touchdown during running the hip is flexed at 30-40°, while also being
209 externally rotated, and at push off it is extended and internally rotated (Slocum and
210 James, 1968). **Furthermore**, during running (3.5m/s), loads have been shown to
211 increase to greater than double that of walking (1.5 m/s) (van den Bogert et al.1999).

212
213 [Insert **Figure 1** about here]
214

215 Great apes and humans vary in the external morphology of the hip joint.
216 Chimpanzees and gorillas have a relatively small femoral head, a short femoral neck
217 **as well as** a superoinferiorly expanded greater trochanter compared to orangutans
218 (McHenry and Corruccini, 1978; Harmon, 2007). Chimpanzees have a “laterally facing
219 acetabulum” (Jenkins, 1972), however comparative quantitative data **of acetabulum**
220 **anteversion do not exist for apes and humans** (Hogervorst et al. 2009 and references
221 therein). Furthermore, in gorillas the acetabulum is relatively deep, compared to
222 other apes (Schultz, 1969), perhaps reducing capacity for mobility at the hip. In
223 orangutans the greater trochanter is less superoinferiorly expanded than in the
224 African apes and is positioned inferiorly to the femoral head, which may enhance
225 rotational capacity at the hip joint (Aiello and Dean, 2002; Harmon 2007). Orangutans
226 also **have** a relatively large head, long neck, and a greater trochanter that is less
227 superoinferiorly expanded than that of African apes and which is **positioned** inferiorly
228 relative to the femoral head (Aiello and Dean, 2002; Harmon, 2007). **These features of**
229 **the orangutan proximal femur, plus the absence of a subchondral ligamentum teres**
230 **insertion at the centre of the femoral head (Crelin, 1988; Ward, 1991; Ruff, 2002;**
231 **Harmon, 2007), enhance rotational capacity and allow greater mobility at the hip**
232 **joint compared to other hominoids.**

233
234 Humans have a long femoral neck and a valgus angle at the knee, which compensate
235 for the mechanical disadvantage of increased bi-acetabular distance (Lovejoy, 1975;
236 McHenry and Corruccini, 1978; Rafferty, 1998; Lovejoy et al. 2002; Harmon, 2007) and
237 result in adduction of the hips during the stance phase (O’Neill et al. 2015). The
238 greater trochanter is less superoinferiorly expanded compared to other apes
239 (Harmon, 2007). Furthermore, the human acetabulum is relatively deep and the
240 femoral head is relatively large (Schultz, 1969; Jungers, 1988). This hip morphology is
241 thought to help dissipate the increased load that occurs when supporting body mass
242 over two, rather than four, limbs. Biomechanical studies have revealed **that** the peak
243 contact force on the human hip during walking is directed posteriorly, laterally and

244 inferiorly (Pedersen et al. 1997) and is located at the posterior aspect (Paul, 1976;
245 English and Kilvington, 1979). Furthermore, pressure on the acetabulum is mainly
246 located posteriorly during different activities, such as standing up or sitting down
247 (Yoshida et al. 2006). Lack of congruence between the femoral head and the
248 acetabulum, combined with an anterior-facing acetabulum result in the anterior
249 region of the femoral head not being fully covered by the acetabulum during bipedal
250 locomotion (Hogervorst et al. 2009; Bonneau et al. 2014). Thus, the anterior region of
251 the femoral head and acetabulum play a smaller role in load transmission compared
252 to other regions of the hip joint.

253

254 Examining the potential links between internal femoral bone structure and extant ape
255 locomotion will greatly facilitate attempts to reconstruct the locomotion of extinct
256 hominins (e.g. Skinner et al. 2015). Here we provide this comparative context by
257 analysing the trabecular architecture throughout the entire femoral head in extant
258 great apes and humans that vary in their locomotor behaviours. We quantify BV/TV,
259 DA, trabecular number (Tb.N), trabecular separation (Tb.Sp) and trabecular thickness
260 (Tb.Th) throughout the femoral head. Based on the locomotor and biomechanical
261 studies reviewed above, we make the following predictions regarding species
262 variation in femoral head trabecular structure:

263

264 *1. BV/TV distribution in the femoral head*

265

266 The distribution of BV/TV throughout the femoral head will reflect joint positioning
267 and loading during habitual locomotion. In *Pan* we expect high BV/TV to extend
268 from the posterior and superior aspect of the femoral head to the anterior region,
269 reflecting hip angles and loading during knuckle-walking locomotion and vertical
270 climbing (Finestone et al. 2018; Isler 2005). We predict that *Gorilla* will show a similar
271 pattern of BV/TV distribution, although the region of high BV/TV is expected to
272 extend over a smaller area of the femoral head compared with that of *Pan*, reflecting
273 a reduced range of motion (Hammond, 2014) and different flexion/extension angles
274 at the *Gorilla* hip during knuckle-walking and climbing (Finestone et al. 2018; Isler
275 2005). We predict that *Pongo* will show the most variable BV/TV distribution pattern,
276 reflecting loading of the femoral head at different hip joint angles, with high BV/TV
277 spanning the whole of the superior area of the femoral head. Finally, we expect a
278 more restricted region of high BV/TV in *Homo* that will be concentrated superiorly
279 and posteriorly on the femoral head, reflecting the stereotypical loading pattern of
280 bipedal locomotion.

281

282 *2. Mean trabecular parameters in the femoral head*

283

284 We hypothesise that relative interspecific differences in mean BV/TV values will be
285 consistent with those of previous trabecular studies on the femur (e.g. Georgiou et al.
286 2018; Ryan et al. 2018; Tsegai et al. 2018) and other postcranial elements (e.g. Maga

287 et al. 2006; Cotter et al. 2009; Scherf et al. 2013; Tsegai et al. 2013; Tsegai et al. 2017),
288 such that *Pan* will have the highest BV/TV, *Homo* will have the lowest, and *Gorilla* and
289 *Pongo* will be intermediate between these two taxa. Furthermore, mean DA of the
290 entire femoral head will reflect the range of motion of the hip joint during habitual
291 locomotion. *Pan* and *Gorilla* will display intermediate DA values, showing less
292 anisotropic femoral heads than *Homo*, because they engage in both terrestrial and
293 arboreal behaviours that employ an increased range of motion at the hip. *Pongo* will
294 be the most isotropic, reflecting their highly mobile hip joint and diverse positioning
295 of the proximal femur during their varied quadrumanous locomotor behaviours.
296 *Homo* will be the most anisotropic, consistent with more stereotypical loading of the
297 hip joint during bipedal locomotion.

298
299 In addition to BV/TV and DA, we quantify mean Tb.N, Tb.Sp and Tb.Th within the
300 femoral head to better understand potential variation in the trabecular architecture
301 across our sample and for comparison with previous studies (e.g. Ryan and Shaw,
302 2012; Ryan and Shaw, 2015; Ryan et al. 2018). In primates these parameters scale
303 negatively allometrically with body size (Barak et al. 2013; Ryan and Shaw, 2013)
304 meaning results may be affected by body mass. BV/TV and DA are expected to better
305 reflect functional adaptations, as DA does not to scale with body mass and BV/TV
306 either shows no relationship (Doube et al. 2011; Barak et al. 2013) or a weak
307 positively allometric relationship (Ryan and Shaw, 2013) with body mass.

308

309

310 **Methodology**

311

312 *Study sample*

313

314 Microcomputed tomographic scans were used to analyse trabecular morphology in
315 the femoral head of great apes and humans. Details of the study sample are
316 provided in Table 1. The *P. troglodytes* sample (n=20) is comprised of two subspecies;
317 *Pan troglodytes verus* (n=15) from the Tai Forest collection curated at the Max Planck
318 Institute for Evolutionary Anthropology in Leipzig, Germany, and *Pan troglodytes*
319 *troglodytes* (n=5) curated at the Smithsonian National Museum of Natural History in
320 Washington, D.C., USA. The *Gorilla gorilla gorilla* sample (n=14) is from the Powell-
321 Cotton Museum, UK, of which 13 individuals are from Cameroon and one is from the
322 Democratic Republic of the Congo. The *Pongo* sample (n=5 and all female) is from
323 the Zoologische Staatssammlung München, Germany. Four of the individuals are *P.*
324 *pygmaeus*, while one is *P. abelii*. The *H. sapiens* sample (n=12) is curated at the
325 Georg-August-Universität Göttingen, Germany. Ten of the individuals come from a
326 Catholic cemetery in Göttingen, which was used between 1851 and 1889, and two
327 come from a cemetery in the village of Inden that was used between 1877 and 1924.
328 All specimens were adult based on complete epiphyseal fusion throughout the
329 skeleton and none showed obvious signs of pathology.

330

331 The *Pan*, *Pongo* and *Homo* samples were scanned at the Department of Human
332 Evolution in the Max Planck Institute for Evolutionary Anthropology, Leipzig,
333 Germany using a BIR ACTIS 225/300 industrial microCT scanner. The *Gorilla* sample
334 was scanned at the Cambridge Biotomography Centre in the Department of Zoology
335 at the University of Cambridge, Cambridge, UK using a Nikon XT 225 ST microCT
336 scanner. All specimens were scanned at the highest possible resolution based on the
337 size of the bone, ranging from 0.029-0.082 mm, and were reconstructed into 16-bit
338 TIFF stacks with isometric voxel sizes. Reconstructed datasets were re-oriented to the
339 same anatomical position and cropped in AVIZO 6.3 ® (Visualization Sciences Group,
340 SAS). All specimens, except six gorillas, were re-sampled due to computational
341 limitations of medtool 4.1 (www.dr-pahr.at) and resultant resolutions are given in
342 Table 1. Bone was segmented from air using the Ray Casting Algorithm (Scherf and
343 Tilgner, 2009).

344

345 *Trabecular architecture analysis*

346

347 Patterns of trabecular bone distribution throughout the whole femoral head were
348 analysed in medtool 4.1 (www.dr-pahr.at), following the protocol described by Gross
349 and colleagues (2014). A series of morphological filters were applied to identify and
350 remove the cortical shell, thus isolating the trabecular structure. The resulting
351 isolated trabecular structure was used to calculate trabecular thickness using the
352 BoneJ plug-in (version 1.4.1, Doube et al. 2010) for ImageJ (Schneider et al. 2012) to
353 validate the parameters used in the morphological filters for the separation of the
354 cortical shell (see Gross et al. 2014). The original dataset and trabecular structure
355 were used to create a trinary mask defining the outer air, inner air and trabecular
356 bone. A 3D rectangular background grid with a size of 3.5mm was superimposed on
357 the trabecular structure and a sphere with a diameter of 7.5mm was used to measure
358 BV/TV at each node in medtool 4.1. BV/TV was calculated as the ratio of bone to
359 total volume in the sampling spheres. The isolated trabecular structure and a mesh
360 size of 0.6mm were used to create 3D tetrahedral meshes of all individuals, using
361 CGAL 4.4 (CGAL, Computational Geometry, <http://www.cgal.org>) and BV/TV values
362 were then interpolated on the tetrahedral elements of each mesh. Distribution maps
363 of BV/TV were visualised using Paraview v4.0.1 (Ahrens et al. 2005). The femoral head
364 for each specimen was manually isolated in AVIZO 6.3 ® by positioning the
365 mediolateral axis facing superoinferiorly and cropping at the head-neck junction to
366 ensure homology across specimens. Trabecular parameters (BV/TV, DA, Tb.N, Tb.Sp,
367 Tb.Th) for the femoral head were calculated using an in-house script in medtool 4.1.
368 Mean BV/TV, DA, Tb.Sp and Tb.Th were quantified within the entire epiphysis and
369 Tb.N was calculated from the means of Tb.Sp and Tb.Th. DA was calculated as $DA = 1$
370 $- [\text{smallest eigenvalue}/\text{largest eigenvalue}]$, as they were calculated using the mean-
371 intercept-length method (Whitehouse, 1974; Odgaard, 1997). Tb.Sp and Tb.Th were

372 calculated based on the Hildebrand and Ruesegger (1997) method; Tb.N was then
373 calculated as $Tb.N = 1 / (Tb.Th + Tb.Sp)$.

374

375 *Statistical analysis*

376

377 Statistical analysis was performed in R v3.4.1 (R Core Team, 2017). The Kruskal-Wallis
378 test was used to evaluate interspecies differences in mean trabecular parameters
379 (BV/TV, DA, Tb.N, Tb.Sp, Tb.Th) of the femoral head and a Wilcoxon rank sum test
380 with Bonferroni correction was used for post-hoc pairwise comparisons.

381

382

383 **Results**

384

385 *BV/TV distribution in the femoral head*

386

387 In *Pan*, BV/TV distribution maps of the femoral head reveal concentrations of high
388 BV/TV in the superior aspect of the femoral head (Fig. 2). In most *Pan* individuals
389 (n=12) there are two distinct concentrations, one located more posteriorly and one
390 located more anteriorly, whereas in some individuals one concentration spans the
391 whole of the superior region of the articulation. While the posterior concentration is
392 always present in *Pan*, the location, extent and isolation of the anterior concentration
393 varies between individuals.

394

395 [Insert **Figure 2** about here]

396

397 The pattern of BV/TV distribution in *Gorilla* is similar to that found in *Pan* (Fig. 3).
398 Two concentrations of high BV/TV are seen in the superior aspect, one located
399 anteriorly, and one located posteriorly. Unlike in *Pan* however, these concentrations
400 are distinct from each other in all but three *Gorilla* individuals, in which a region of
401 high BV/TV spans across the superior region of the femoral head. There is no
402 apparent difference in the size of the two regions of high BV/TV.

403

404 [Insert **Figure 3** about here]

405

406 *Pongo* shows a slightly different BV/TV pattern compared to *Pan* and *Gorilla* (Fig. 4).
407 The *P. pygmaeus* individuals show the two concentrations of high BV/TV, one in the
408 anterior and one in the posterior, similar to what is found in the African apes,
409 however intermediate values persist over the superior portion of the femoral head.
410 The extent of this concentration differs between *P. pygmaeus* individuals: in two
411 individuals it is restricted more in the superior aspect of the head, whereas in the
412 other two it is enlarged and covers the majority of the femoral head, from the
413 anterior to the posterior. When the two concentrations are more well-defined, the
414 posterior concentration is generally more mediolaterally expanded than the anterior

415 concentration. The *P. abelii* individual shows lower BV/TV than the other specimens
416 and does not show two distinct concentrations.

417

418 [Insert **Figure 4** about here]

419

420 *Homo* shows a different pattern to the great apes (Fig. 5). All individuals show one
421 region of high BV/TV located in the posterior and superior aspect of the femoral
422 head. Intermediate values of BV/TV expand across the whole of the superior aspect
423 of the head of *Homo*, but with no apparent second concentration of high BV/TV in
424 the anterior region as found in great apes. *Homo* individuals also display
425 intermediate BV/TV on the inferior aspect of the head. This expansion of
426 intermediate BV/TV values along the inferior is not seen in the other apes.

427

428 [Insert **Figure 5** about here]

429

430

431 *Quantitative analysis of trabecular parameters in the femoral head*

432

433 Quantitative analysis of the mean trabecular parameters over the femoral head
434 revealed several differences across taxa. Results for each parameter in the different
435 taxa are presented in Table 2 and statistical results of species pairwise comparisons,
436 after Bonferroni corrections, are presented in Table 3. *Pan* shows significantly higher
437 BV/TV in the femoral head than *Pongo* ($p=0.05$) and *Homo* ($p<0.001$), and although
438 its mean BV/TV value was higher than that of *Gorilla*, this difference was not
439 statistically significant (Tables 2 and 3). *Homo* has the lowest mean BV/TV compared
440 with all the great apes but is only significantly different from *Pan*. *Homo* has
441 significantly higher DA in the femoral head than all other apes (*Pan* $p<0.001$; *Gorilla*
442 $p<0.05$; *Pongo* $p<0.01$), while *Pan*, *Pongo* and, less so, *Gorilla* are more isotropic and
443 not significantly different from each other. With regards to the architectural
444 parameters, *Pan* shows the most distinct trabecular structure with significantly higher
445 Tb.N than all other apes (*Gorilla* $p<0.001$; *Homo* $p<0.001$; *Pongo* $p<0.01$) and
446 significantly lower Tb.Sp (all $p<0.001$) and lower Tb.Th than *Gorilla* ($p<0.001$) and
447 *Homo* ($p<0.05$).

448

449 Differences in mean BV/TV and DA across taxa were further evaluated using a
450 bivariate plot (Fig.6) and a line histogram of the distribution of values in each taxon
451 (Fig. 7). The data depicted in these figures are mean values for each individual across
452 the entire femoral head. In the bivariate plot *Pan* shows a combination of high BV/TV
453 and low DA, in contrast to humans that show the opposite pattern. *Gorilla* overlaps
454 with both of these taxa but shows higher BV/TV than humans. *Pongo* individuals
455 overlap with the African apes, with lower DA values than humans, but with BV/TV
456 values that overlap with all other taxa.

457

458 [Insert **Figure 6** about here]

459

460 These differences are reflected in the distribution of BV/TV and DA values in the taxa
461 (Fig. 7). *Pan* shows the highest mean BV/TV and **most individuals** close to the mean
462 (0.39), whereas *Gorilla* shows a lower mean value but **most individuals** between 0.3
463 and 0.4. *Pongo* shows a similar mean to *Gorilla*, however the distribution of values
464 **more greatly resembles** that of *Pan*. *Homo* shows the lowest BV/TV values distributed
465 over a wider area. The DA plot shows that *Pan*, *Gorilla* and *Pongo* present similarly
466 low mean DA values, but *Pongo* differs in distribution with **more individuals** around
467 the mean. *Homo* shows a different distribution with the highest mean DA but a wider
468 distribution of values in the sample.

469

470 [Insert **Figure 7** about here]

471

472

473 **Discussion**

474

475 Our study investigated the variation in trabecular patterns of the femoral head in
476 great apes and humans. Qualitative and quantitative results supported our
477 hypotheses that trabecular bone would reflect differences in locomotor patterns, but
478 not necessarily in the way we predicted. *Pan* and *Gorilla* displayed trabecular
479 structures consistent with their terrestrial as well as arboreal quadrupedal
480 locomotion, while *Homo* showed a distinct trabecular pattern indicative of
481 stereotypical loading during bipedal locomotion. However, the African apes showed
482 a BV/TV distribution pattern that was **different to what was expected**, and their
483 trabecular structure did not differ significantly from *Pongo*.

484

485 *Distribution of BV/TV within the femoral head*

486

487 We predicted that African apes would display a region of high BV/TV extending from
488 the posterosuperior to the anterior region of the femoral head, reflecting the flexed
489 hip postures and loading incurred during knuckle-walking and vertical climbing.
490 However, instead of a continuous band of high BV/TV across the femoral head, *Pan*
491 displayed two main regions of high BV/TV, indicating two regions of high loading;
492 one in the **posterosuperior** aspect of the femoral head and one located more
493 anteriorly. The majority of Tai chimpanzee (75% of the *Pan* sample) locomotion is
494 terrestrial quadrupedalism (Doran, 1993). Ground reaction forces remain high
495 throughout the stance phase during terrestrial knuckle-walking (Barak et al. 2013)
496 and the hip remains flexed (Finestone et al. 2018), both of which are consistent with
497 high loading of the posterosuperior region of the femoral head and the high BV/TV
498 concentration that was found in this region. While Tai chimpanzees engage less
499 frequently in vertical climbing (Doran, 1993a), it is possible that this results in
500 similarly high loading of the femoral head, **as it involves high propulsive forces from**

501 **the hindlimbs** (Hanna et al. 2017). During climbing, the hip can be flexed to a
502 maximum of 25° to 55° (Isler, 2005; Nakano et al. 2006), which would result in the
503 anterior aspect of the head contacting the lunate surface of the acetabulum. This is
504 consistent with the second region of high BV/TV found in the anterior portion of the
505 femoral head **in Pan**. The anterior concentration was more variable between
506 individuals, but **this** could not be explained by subspecies differences within the
507 sample. Thus, the more variable anterior BV/TV pattern may reflect interindividual
508 variability in vertical climbing frequency (Doran, 1993b) or hip range of motion
509 during climbing (Isler, 2005; Nakano et al. 2006).

510

511 *Gorilla* displayed a similar pattern to *Pan*, with two regions of high BV/TV within the
512 femoral head. The two regions, one in the posterior and one in the anterior aspect of
513 the head, are, as in *Pan*, consistent with hip posture and loading during terrestrial
514 quadrupedalism and vertical climbing, as these modes of locomotion comprise the
515 majority of *Gorilla* locomotion (Doran, 1997; Crompton et al. 2010; Remis, 1995).
516 However, unlike *Pan*, these regions were better defined and more discrete in most
517 *Gorilla* individuals (**11 out of 14 individuals**). This more discrete pattern is perhaps
518 due to their greater body mass. Greater mass is related to restricted range of motion
519 in joints (Hammond, 2014), which could result in less variability in joint positioning
520 during locomotion and may explain the more **well-defined** concentrations in *Gorilla*.
521 The two concentrations appeared closer to each other in *Gorilla* than in *Pan*, which is
522 also consistent with the reduced range of motion at the hip joint of *Gorilla* (Isler,
523 2005; Hammond, 2014). Significant sex and body size related differences in joint
524 mobility are prominent in *Gorilla*, with females showing a larger range **of motion**
525 **than** males and flexion-extension ranges varying between the sexes by up to or even
526 more than 30° (Isler, 2005; Hammond, 2014). These differences were not detected in
527 the BV/TV distribution maps and *Gorilla* does not seem to be more variable than
528 *Pan*. However, this could not be tested statistically in the current study.

529

530 We predicted that the BV/TV distribution pattern of the *Pongo* femoral head would
531 differ from that of African apes and humans because of their more varied
532 quadrumanous locomotor behaviours (Thorpe and Crompton, 2005; Thorpe and
533 Crompton, 2006), more mobile hip joints (Crelin, 1988; Ward, 1991), and increased
534 range of motion at the hip during vertical climbing compared to African apes (Isler,
535 2005). Four of the five *Pongo* individuals in our sample showed the same two regions
536 of high BV/TV found in African apes, however these were not as distinct and, instead,
537 there was a continuous concentration of BV/TV spanning the superior aspect of the
538 femoral head. This is perhaps unsurprising since *Pongo* uses a variety of hip postures
539 while navigating their arboreal environment (Thorpe and Crompton, 2005; Thorpe
540 and Crompton, 2006; Payne et al. 2006; Thorpe et al. 2009), which potentially results
541 in higher loading across the whole superior surface of the femoral head. *Pongo* also
542 vertically climbs less frequently than African apes (Thorpe and Crompton, 2006),
543 which may be **reflected by** the less defined anterior concentration of high BV/TV in

544 *Pongo* compared with *Pan* and, especially, with *Gorilla*. Although our sample of
545 *Pongo* is small (n=5) and all individuals were female, there was greater variation in
546 the BV/TV distributions along the anterior and posterior aspects of the femoral head
547 than was found in African apes. The one *P. abelii* specimen in our sample differed
548 from the *P. pygmaeus* individuals in having only one superior concentration of high
549 BV/TV. Although locomotor differences have been documented between *P.*
550 *pygmaeus* and *P. abelii* (Sugardjito and van Hooff, 1986; Cant, 1987), a larger sample
551 of both species is needed to determine if this variation in the trabecular pattern is
552 characteristic of each species.

553

554 *Homo* showed a distinct trabecular pattern that is consistent with our predictions and
555 similar to previous results showing the density distribution of trabeculae adjacent to
556 cortical bone (Treece and Gee, 2014). All *Homo* individuals displayed one main region
557 of high BV/TV, located posteriorly and superiorly on the femoral head. This
558 concentration was positioned more medially than the posterior concentration seen in
559 great apes and closer to the fovea capitis, which is consistent with loading of the
560 femur at a valgus angle. Intermediate BV/TV values continued along the superior
561 aspect of the femoral head in *Homo*. This is consistent with loading that occurs
562 throughout the gait cycle over the articulating surface but suggests that peak
563 loading is occurring at the posterosuperior region, which is in contact with the
564 acetabulum during walking (Bonneau et al. 2012; Bonneau et al. 2014). Of course,
565 humans also engage in other activities that involve more flexed hip joint postures,
566 such as running, jumping, or climbing stairs, all of which impose high loads on the
567 lower limb (van den Bogert et al. 1999; Giarmatzis et al. 2015) and could result in
568 some trabecular reorganisation, explaining the extended area of intermediate BV/TV
569 values we found across the femoral head. Unfortunately, it is not yet known exactly
570 how the peak load is distributed over the femoral head during these activities.
571 However, all individuals lack the anterior concentration found in apes, further
572 supporting the interpretation that high BV/TV in the anterior region could be linked
573 to arboreal behaviours or more specifically vertical climbing.

574

575 *Quantitative analysis of trabecular structure*

576

577 Quantitative analysis of the femoral head trabecular structure only partially
578 supported our hypotheses. As expected, *Homo* displayed the lowest mean BV/TV in
579 our sample but was only significantly different from that of *Pan*. Our results confirm
580 previous studies showing that modern humans, particularly those that are less active,
581 have relatively lower BV/TV across the skeleton compared with highly mobile modern
582 humans and other primates (Chirchir et al. 2015; Ryan and Shaw, 2015; Saers et al.
583 2016; Chirchir et al. 2017). Furthermore, *Homo* showed significantly higher DA than
584 great apes, which is consistent with the more stereotypical loading of the hip joint
585 during bipedal locomotion and in accordance with previous results from the proximal
586 (Ryan and Shaw, 2015; Ryan et al. 2018) as well as the distal femur (Georgiou et al.

587 2018). *Homo* has narrower acetabulae than other great apes, with expanded cranial
588 lunate surfaces, as well as shortened dorsal surfaces, which result in a distinctively-
589 shaped dorso-cranially expanded lunate surface that may restrict movement in the
590 parasagittal plane (San Millán et al. 2015). Furthermore, in *Homo* the iliofemoral
591 ligament limits extension and external rotation (Myers et al. 2011), the ischiofemoral
592 ligament limits internal rotation and the pubofemoral ligament limits abduction
593 (Wagner et al. 2012), all of which result in a more restrictive and stereotypical motion
594 and loading of the femoral head that is reflected in the trabecular structure.

595

596 As predicted, mean BV/TV was highest in *Pan*, which is consistent with previous
597 studies showing relatively high BV/TV in the African ape femur (Ryan and Shaw, 2015;
598 Georgiou et al. 2018; Ryan et al. 2018; Tsegai et al. 2018) and other postcranial
599 elements (e.g. Cotter et al. 2009; Scherf et al. 2013; Tsegai et al. 2017). BV/TV in *Pan*
600 did not differ significantly from *Gorilla*, reflecting their generally similar locomotor
601 repertoire. Overall, the quantitative analysis highlighted *Pan* as being distinct from
602 the other taxa. *Pan* not only showed the highest BV/TV values, but also differed
603 significantly from all taxa in Tb.N and Tb.Sp, showing consistently higher Tb.N and
604 lower Tb.Sp, again resembling previous findings (Ryan and Shaw, 2015). Furthermore,
605 *Pan* showed significantly lower Tb.Th than *Gorilla* and *Homo*. Additionally, mean DA
606 was lowest in *Pan*, as well as *Pongo*, but only differed significantly from *Homo*. Less
607 data is available on the femoral ligaments of non-human apes however *Pan* and
608 *Pongo* seem to have less restrictive ligaments than *Homo* (Sonntag, 1923; 1924).

609

610 The trabecular structure of *Gorilla* and *Pongo* was not as distinct. *Gorilla* mean BV/TV
611 did not differ significantly from any other taxon, and they only differed significantly
612 in Tb.N, Tb.Sp and Tb.Th from *Pan*, as well as in DA from *Homo*. *Gorilla* has less
613 variable positioning of their lower limbs during locomotion, compared to other non-
614 human apes, as was shown in vertical climbing (Isler, 2005), however this is not
615 displayed as clearly in their DA values as was initially predicted. The lack of significant
616 differences in BV/TV and DA with *Pan* can perhaps be explained by the similar shape
617 of their hip joints (San Millán et al. 2015) and overall similarities in locomotion
618 (Doran, 1997). None of great apes differed significantly in DA, despite clear
619 differences in locomotor behaviours and hip morphology. *Pongo* has a cranio-
620 ventrally expanded lunate surface and a smaller acetabular fossa than other apes.
621 They also show the largest articular surfaces and relatively shallow acetabulae
622 (Schultz, 1969), which may be responsible for the increased mobility of the femoral
623 head. Furthermore, *Pongo* has a greater capacity for abduction and external rotation
624 than non-suspensory taxa (Hammond, 2014). Thus, *Pongo* was expected to display
625 significantly lower DA values than all other taxa, which was not the case, but this
626 result may also reflect our small sample size for this taxon.

627

628 Our results showed that *Pan* has relatively numerous, thinner and compactly
629 organised trabeculae, while *Gorilla* and *Homo* have relatively few, thicker and more

630 separated trabeculae. *Pongo* has relatively few, thinner and more separated
631 trabeculae. These results are largely in accordance with previous analyses of femoral
632 head trabeculae (Ryan and Shaw, 2012; 2015) which showed that humans have
633 relatively less numerous, thin and highly anisotropic trabeculae compared to other
634 anthropoids, *Pan* have relatively high numbers of thick, isotropic trabeculae and
635 *Pongo* have relatively few, isotropic trabeculae. *Gorilla* showed the thickest
636 trabeculae (Table 2), in support of previous studies suggesting that larger taxa have
637 absolutely thicker trabeculae (Barak et al. 2013; Ryan and Shaw, 2013; Tsegai et al.
638 2013). However, the difference was not found to be significant, possibly due to the
639 small sample sizes in our study. Allometric relationships were not tested in our study
640 because our sample sizes were not large enough to test this intraspecifically,
641 however previous research has shown that these trabecular parameters can vary
642 predictably with body size interspecifically (Cotter et al. 2009; Doube et al. 2011;
643 Barak et al. 2013; Ryan and Shaw, 2013). Across a large sample of mammals, Tb.Th
644 and Tb.Sp were shown to increase with size (Doube et al. 2011). In primates, Tb.N,
645 Tb.Th and Tb.Sp present negatively allometric relationships with body mass (Barak et
646 al. 2013; Ryan and Shaw, 2013), resulting in more, thinner and less separated
647 trabeculae in larger taxa. These studies suggest that absolute trabecular parameters,
648 and specifically Tb.N, Tb.Sp and Tb.Th, do not necessarily directly reflect locomotor
649 modes as they could reflect body-size related or systemic differences between taxa.
650 Nevertheless, since our sample includes apes that are relatively similar in body size
651 compared to the more diverse samples of previous studies (Doube et al. 2011; Barak
652 et al. 2013; Ryan and Shaw, 2013), we would expect that allometry does not have a
653 significant effect on the variation observed here.

654
655 The absence of a clear functional signal in the mean trabecular parameters may be
656 due to methodological limitations of the whole-epiphysis approach. The mean value
657 of any given trabecular parameter can obscure or homogenise any potential distinct
658 variation in specific regions of the femoral head, as demonstrated by the BV/TV
659 distribution maps and previous studies (Sylvester and Terhune, 2017). This is where
660 the traditional VOI approach, in which the trabecular architecture of specific regions
661 of an epiphysis can be quantified and compared, is potentially more functionally
662 informative (e.g. Ryan and Shaw, 2012; 2015; Ryan et al. 2018). Additionally, the lack
663 of a strong functional signal in these parameters could be due to non-mechanical
664 factors affecting trabecular structure. Trabecular bone also functions as a reserve of
665 minerals and is important in maintaining homeostasis, hence its structure will, to
666 some extent, be affected by this (Rodan, 1998; Clarke, 2008). Genes control for the
667 rate of remodelling and bone mineral density, as well as the response to mechanical
668 strain in different skeletal sites (Smith et al. 1973; Dequeker et al. 1987; Kelly et al.
669 1991; Garnero et al. 1996; Hauser et al. 1997; Judex et al. 2002; Judex et al. 2004).
670 These factors, along with the fact that trabecular bone remodels in response to a
671 range of magnitudes and frequencies of load (Whalen et al. 1988; Rubin et al. 1990;
672 Rubin et al. 2001; Judex et al. 2003; Scherf et al. 2013), complicate interpretations.

673 Age, hormones, sex and other factors (e.g. Simkin et al. 1987; Pearson and
674 Lieberman, 2004; Suuriniemi et al. 2004; Kivell, 2016; Wallace et al. 2017; Tsegai et al.
675 2018) influence trabecular bone modelling, thus these factors should not be ignored.
676 **Nonetheless, future research will aim to use techniques that will allow statistical**
677 **comparisons of the trabecular distribution patterns in the femoral head of apes,**
678 **rather than mean parameters, for more accurate interpretation of locomotor patterns**
679 **in extinct hominins.**

680

681 **Conclusion**

682

683 **This study showed that** the trabecular architecture of the femoral head in **great apes**
684 **and humans** reflects habitual **hip** postures during locomotion. *Pan* and *Gorilla*
685 **showed** similar BV/TV distribution patterns, **with generally two distinct high BV/TV**
686 **regions that are consistent with hip postures during knuckle-walking and vertical**
687 **climbing.** *Pongo* **showed a BV/TV distribution pattern that is characteristic of their**
688 highly mobile hips and complex locomotion, however **they** do not differ as
689 significantly as predicted **from** African apes. Finally, *Homo* **showed** a distinct pattern
690 of BV/TV distribution, **with one posterosuperior region of high BV/TV,** the lowest
691 overall BV/TV values and highest DA values, **which is** consistent with stereotypical
692 loading during locomotion. **Despite mean trabecular parameters not demonstrating**
693 **locomotor differences as clearly as predicted, they largely match results from**
694 **previous VOI studies (Ryan and Shaw, 2015; Ryan et al. 2018). Our research reveals**
695 **that there are distinct patterns of BV/TV distribution that generally distinguish the**
696 **locomotor groups and provide a** valuable comparative sample for future research on
697 the evolution of gait in hominins.

698

699 **Acknowledgements**

700

701 We thank the following researchers for access to specimens: Anneke Van Heteren
702 (Zoologische Staatssammlung München), Inbal Livne (Powell-Cotton Museum),
703 Christophe Boesch and Jean-Jacques Hublin (Max Planck Institute for Evolutionary
704 Anthropology), and Brigit Grosskopf (Georg-August University of Goettingen). We
705 also thank David Plotzki (Max Planck Institute for Evolutionary Anthropology) and
706 Keturah Smithson (University of Cambridge) for the CT scanning of specimens. We
707 thank Zewdi Tsegai for facilitating access to CT data and Kim Deckers for discussions
708 that improved this manuscript. **We are grateful to two anonymous reviewers for their**
709 **valuable feedback that improved this manuscript.** This research is supported by a
710 50th Anniversary Research Scholarship, University of Kent (LG), European Research
711 Council Starting Grant 336301 (MMS, TLK), and the Max Planck Society (MMS, TLK).

712

713

714 **Author contributions**

715

716 L. Georgiou, T.L. Kivell and M.M. Skinner contributed to the design of the study and
717 acquisition of data, **L. T. Buck facilitated and collected data**, D.H Pahr contributed to
718 the analysis tools, L. Georgiou processed, analysed and interpreted the data, L.
719 Georgiou drafted the manuscript, L. Georgiou, T.L. Kivell, D.H. Pahr, **L.T. Buck** and
720 M.M. Skinner revised and approved the final manuscript submitted for review.
721

722

723 **References**

724

725 **Abbass SJ, Abdulrahman G** (2014) Kinematic Analysis of Human Gait Cycle. *Nahrain*
726 *University College of Engineering Journal (NUCEJ)* **16**, (2), 208-222.

727 **Ahrens J, Geveci B, Law C** (2005) ParaView: An end-user tool for large data
728 visualization. in Hansen CD, Johnson CR (eds). *Visualization handbook*. Butterworth-
729 Heinemann, Burlington. MA, 717-731.

730 **Aiello I, Dean C** (2002) *An Introduction to Human Evolutionary Anatomy*. Academic
731 Press, San Diego.

732 **Alexander CJ** (1994) Utilisation of joint movement range in arboreal primates
733 compared with human subjects: an evolutionary frame for primary osteoarthritis.
734 *Annals of the Rheumatic Diseases* **53** (11), 720-725.

735 **Barak MM, Lieberman DE, Hublin J** (2011) A Wolff in sheep's clothing: Trabecular
736 bone adaptation in response to changes in joint loading orientation. *Bone* **49** (6),
737 1141-1151.

738 **Barak MM, Lieberman DE, Hublin J** (2013) Of mice rats and men: Trabecular bone
739 architecture in mammals scales to body mass with negative allometry. *Journal of*
740 *Structural Biology* **183** (2), 123-131

741 **Barak MM, Lieberman DE, Raichlen D, et al.** (2013) Trabecular Evidence for a
742 Human-Like Gait in *Australopithecus africanus*. *PLOS ONE* **8** (11), e77687

743 **Biewener AA, Fazzalari NL, Konieczynski DD, et al.** (1996) Adaptive changes in
744 trabecular architecture in relation to functional strain patterns and disuse. *Bone* **19**, 1-
745 8.

746 **Bonneau N, Baylac M, Gagey O, et al.** (2014) Functional integrative analysis of the
747 human hip joint: The three-dimensional orientation of the acetabulum and its
748 relation with the orientation of the femoral neck. *The Journal of Human Evolution* **69**,
749 55-69.

750 **Bonneau N, Gagey O, Tardieu C** (2012) Biomechanics of the human hip joint.
751 *Computer Methods in Biomechanics and Biomedical Engineering*, **15**, 197-199.

752 **Burr DB, Piotrowski G, Martin RB, et al.** (1982) Femoral mechanics in the lesser
753 bushbaby (*Galago senegalensis*): Structural adaptations to leaping in primates.
754 *Anatomical Record* **202**, 419-429.

- 755 **Cant JG** (1987) Positional behavior of female bornean orangutans (*Pongo*
756 *pygmaeus*). *American Journal of Primatology* **12** (1), 71-90
- 757 **Carey TS, Crompton RH** (2005) The metabolic costs of 'bent-hip bent-knee' walking
758 in humans. *The Journal of Human Evolution* **48** (1), 25-44.
- 759 **Carlson KJ, Lublinsky S, Judex S** (2008) Do different locomotor modes during
760 growth modulate trabecular architecture in the murine hind limb? *Integrative and*
761 *Comparative Biology* **48** (3), 385-393.
- 762 **Chirchir H, Kivell TL, Ruff CB, et al.** (2015) Recent origin of low trabecular bone
763 density in modern humans. *Proceedings of the National Academy of Sciences* **112** (2),
764 366-371.
- 765 **Chirchir H, Ruff CB, Junno JA, et al.** (2017) Low trabecular bone density in recent
766 sedentary modern humans. *American Journal of Physical Anthropology* **162** (3),
767 e23138.
- 768 **Clarke B** (2008) Normal Bone Anatomy and Physiology. *Clinical Journal of the*
769 *American Society of Nephrology* **3**, 131-139.
- 770 **Cotter MM, Simpson SW, Latimer BM, et al.** (2009) Trabecular Microarchitecture of
771 Hominoid Thoracic Vertebrae. *The Anatomical Record* **292** (8), 1098-1106.
- 772 **Crelin ES** (1988) Ligament of the head of the femur in the orangutan and Indian
773 elephant. *The Yale journal of biology and medicine* **61** (5), 383-388.
- 774 **Crompton RH, Sellers WI, Thorpe SKS** (2010) Arboreality terrestriality and
775 bipedalism. *Philosophical Transactions of the Royal Society B: Biological Sciences* **365**
776 (1556), 3301-3314.
- 777 **Crompton RH, Weijie LYW, Günther M, et al.** (1998) The mechanical effectiveness
778 of erect and) bent-hip bent-knee. bipedal walking in *Australopithecus afarensis*. *The*
779 *Journal of Human Evolution* **35** (1), 55-74.
- 780 **Demes B, Larson SG, Stern JT Jr, et al.** (1994). The kinetics of primate
781 quadrupedalism: "hindlimb drive" reconsidered. *Journal of human evolution* **26**, 353-
782 374.
- 783 **Dequeker J, Nijs J, Verstraeten A, et al.** (1987) Genetic determinants of bone
784 mineral content at the spine and radius: A twin study. *Bone* **8** (4), 207-209.
- 785 **DeSilva JM, Holt KG, Churchill SE, et al.** (2013) The Lower Limb and Mechanics of
786 Walking in *Australopithecus sediba*. *Science* **340**, (6129).
- 787 **Doran DM** (1993a) Comparative locomotor behavior of chimpanzees and bonobos:
788 The influence of morphology on locomotion. *American Journal of Physical*
789 *Anthropology* **91** (1), 83-98.
- 790 **Doran DM** (1993b) Sex differences in adult chimpanzee positional behavior: the
791 influence of body size on locomotion and posture. *American Journal of Physical*
792 *Anthropology* **91**, 99-115.

- 793 **Doran DM** (1997) Ontogeny of locomotion in mountain gorillas and chimpanzees.
794 *Journal of human evolution* **32** (4), 323-344.
- 795 **Doube M, Kłosowski MM, Wiktorowicz-Conroy A, et al.** (2011) Trabecular bone
796 scales allometrically in mammals and birds. *Proceedings of The Royal Society:*
797 *Biological sciences* **278** (1721), 3067-3073
- 798 **Doube M, Kłosowski MM, Arganda-Carreras I, et al.** (2010) BoneJ: Free and
799 extensible bone image analysis in ImageJ. *Bone* **47** (6), 1076-1079
- 800 **English TA, Kilvington M** (1979) In vivo records of hip loads using a femoral implant
801 with telemetric output (a preliminary report). *Journal of Biomedical Engineering* **1** (2),
802 111-115.
- 803 **Fajardo RJ, DeSilva JM, Manoharan RK, et al.** (2013) Lumbar vertebral body bone
804 microstructural scaling in small to medium-sized strepsirhines. *Anatomical Record*
805 **296**, 210-226.
- 806 **Fajardo RJ, Müller R** (2001) Three-dimensional analysis of nonhuman primate
807 trabecular architecture using micro-computed tomography *American Journal of*
808 *Physical Anthropology* **115**, 327-336.
- 809 **Fajardo RJ, Müller R, Ketcham RA, et al.** (2007) Nonhuman anthropoid primate
810 femoral neck trabecular architecture and its relationship to locomotor mode. *The*
811 *Anatomical Record: Advances in Integrative Anatomy and Evolutionary Biology* **290** (4),
812 422-436.
- 813 **Finestone EM, Brown MH, Ross SR, et al.** (2018) Great ape walking kinematics:
814 Implications for hominoid eution. *American Journal of Physical Anthropology* **166** (1),
815 43-55.
- 816 **Garnero P, Arden NK, Griffiths G, et al.** (1996) Genetic influence on bone turnover
817 in postmenopausal twins. *The Journal of Clinical Endocrinology, Metabolism* **81** (1),
818 140-146
- 819 **Giarmatzis G, Ilse J, Mariska W, et al.** (2015) Loading of Hip Measured by Hip
820 Contact Forces at Different Speeds of Walking and Running. *Journal of Bone and*
821 *Mineral Research* **30** (8), 1431-1440.
- 822 **Gross T, Kivell TL, Skinner MM** (2014) A CT-image-based framework for the holistic
823 analysis of cortical and trabecular bone morphology. *Palaeontologia Electronica* **17**
824 (3), 1-13.
- 825 **Gunness-Hey M, Hock JM** (1984) Increased trabecular bone mass in rats treated
826 with human synthetic parathyroid hormone. *Metabolic Bone Disease and Related*
827 *Research* **5** (4), 177-181.
- 828 **Hammond AS** (2014) In vivo baseline measurements of hip joint range of motion in
829 suspensory and nonsuspensory anthropoids. *American Journal of Physical*
830 *Anthropology* **153** (3), 417-434.

- 831 **Hanna JB, Granatosky MC, Rana P, et al.** (2017) The evolution of vertical climbing
832 in primates: Evidence from reaction forces. *Journal of Experimental Biology*
833 <https://doi.org/10.1242/jeb.157628>.
- 834 **Harmon EH** (2007) The shape of the hominoid proximal femur: a geometric
835 morphometric analysis. *Journal of anatomy* **210** (2), 170-185.
- 836 **Harmon EH** (2009a) The shape of the early hominin proximal femur. *American*
837 *Journal of Physical Anthropology* **139** (2), 154-171.
- 838 **Harmon EH** (2009b) Size and shape variation in the proximal femur of
839 *Australopithecus africanus*. *Journal of Human Evolution* **56** (6), 551-559.
- 840 **Harris M, Nguyen TV, Howard GM, et al.** (1998) Genetic and Environmental
841 Correlations Between Bone Formation and Bone Mineral Density: A Twin Study. *Bone*
842 **22** (2), 141-145.
- 843 **Hauser DL, Fox JC, Sukin D, et al.** (1997) Anatomic variation of structural properties
844 of periacetabular bone as a function of age: A quantitative computed tomography
845 study. *The Journal of arthroplasty* **12** (7), 804-811.
- 846 **Havill LM, Allen MR, Bredbenner TL, et al.** (2010) Heritability of lumbar trabecular
847 bone mechanical properties in baboons. *Bone* **46**, 835-840.
- 848 **Hildebrand T, Rüeegsegger P** (1997) A new method for the model-independent
849 assessment of thickness in three-dimensional images. *Journal of microscopy* **185** (1),
850 67-75
- 851 **Hogervorst T, Bouma HW, de Vos J** (2009) Evolution of the hip and pelvis. *Acta*
852 *Orthopaedica* **80**, 1-39.
- 853 **Huiskes R, Ruimerman R, van Lenthe GH, et al.** (2000) Effects of mechanical forces
854 on maintenance and adaptation of form in trabecular bone. *Nature* **405**, 704-706.
- 855 **Hunt KD** (1991) Positional behavior in the Hominoidea. *International Journal of*
856 *Primatology* **12**, 95-118.
- 857 **Isler K, Thorpe SKS** (2003) Gait parameters in vertical climbing of captive
858 rehabilitant and wild Sumatran orang-utans (*Pongo pygmaeus abelii*). *Journal of*
859 *Experimental Biology* **206** (22), 4081-4096.
- 860 **Isler K** (2005) 3D-kinematics of vertical climbing in hominoids. *American Journal of*
861 *Physical Anthropology* **126** (1), 66-81.
- 862 **Jenkins FA** (1972) Chimpanzee Bipedalism: Cineradiographic Analysis and
863 Implications for the Evolution of Gait. *Science* **178** (4063), 877-879.
- 864 **Judex S, Boyd S, Qin Y, et al.** (2003) Adaptations of Trabecular Bone to Low
865 Magnitude Vibrations Result in More Uniform Stress and Strain Under Load. *Annals*
866 *of Biomedical Engineering* **31** (1), 12-20.
- 867 **Judex S, Donahue L, Rubin C** (2002) Genetic predisposition to low bone mass is
868 paralleled by an enhanced sensitivity to signals anabolic to the skeleton. *The FASEB*
869 *Journal* **16** (10), 1280-1282.

- 870 **Judex S, Garman R, Squire M, et al.** (2004) Genetically Based Influences on the Site-
871 Specific Regulation of Trabecular and Cortical Bone Morphology. *Journal of Bone and*
872 *Mineral Research* **19** (4), 600-606.
- 873 **Jungers WL** (1988) Relative joint size and hominoid locomotor adaptations with
874 implications for the evolution of hominid bipedalism. *Journal of Human Evolution* **17**
875 (1-2), 247-265.
- 876 **Keaveny TM, Morgan EF, Niebur GL, et al.** (2001) Biomechanics of trabecular bone.
877 *Annual Review of Biomedical Engineering* **3**, 307-333.
- 878 **Kelly PJ, Hopper JL, Macaskill GT, et al.** (1991) Genetic Factors in Bone Turnover.
879 *The Journal of Clinical Endocrinology and Metabolism* **72** (4), 803-813.
- 880 **Kivell TL** (2016) A review of trabecular bone functional adaptation: what have we
881 learned from trabecular analyses in extant hominoids and what can we apply to
882 fossils? *Journal of anatomy* **228** (4), 569-594.
- 883 **Kivell TL, Skinner MM, Richard L, et al.** (2011) Methodological considerations for
884 analyzing trabecular architecture: an example from the primate hand. *Journal of*
885 *anatomy* **218** (2), 209-225.
- 886 **Lovejoy CO, McCollum MA** (2010) Spinopelvic pathways to bipedality: why
887 (hominids ever relied on a bent-hip-bent-knee gait. *Philosophical Transactions of the*
888 *Royal Society of London B: Biological Sciences* **365** (1556), 3289-3299.
- 889 **Lovejoy CO** (1975) Biomechanical perspectives on the lower limb of early hominids.
890 In Tuttle RH (editor). *Primate Functional Morphology and Evolution*. Mouton, The
891 Hague. 291-326.
- 892 **Lovejoy OC, Meindl RS, Ohman JC, et al.** (2002) The Maka femur and its bearing on
893 the antiquity of human walking: Applying contemporary concepts of morphogenesis
894 to the human fossil record. *American Journal of Physical Anthropology* **119** (2) 97-
895 133.
- 896 **MacLatchy L, Müller R** (2002) A comparison of the femoral head and neck
897 trabecular architecture of Galago and Perodicticus using micro-computed
898 tomography (μ CT). *Journal of Human Evolution* **43** (1), 89-105.
- 899 **Maga M, Kappelman J, Ryan TM, et al.** (2006) Preliminary observations on the
900 calcaneal trabecular microarchitecture of extant large-bodied hominoids. *American*
901 *Journal of Physical Anthropology* **129**, 410-417.
- 902 **Mann RA, Hagy J** (1980) Biomechanics of walking running and sprinting. *The*
903 *American Journal of Sports Medicine* **8** (5), 345-350.
- 904 **McHenry HM, Corruccini RS** (1978) The femur in early human evolution. *American*
905 *Journal of Physical Anthropology* **49** (4), 473-487.
- 906 **Milovanovic P, Danijela D, Michael H, et al.** (2017) Region-dependent patterns of
907 trabecular bone growth in the human proximal femur: A study of 3D bone

- 908 microarchitecture from early postnatal to late childhood period. *American Journal of*
909 *Physical Anthropology* **164** (2), 281-291.
- 910 **Mittra E, Rubin C, Qin Y** (2005) Interrelationship of trabecular mechanical and
911 microstructural properties in sheep trabecular bone. *Journal of Biomechanics* **38**,
912 1229-1237.
- 913 **Miyakoshi N** (2004) Effects of Parathyroid Hormone on Cancellous Bone Mass and
914 Structure in Osteoporosis. *Current Pharmaceutical Design* **10** (21), 2615-2627.
- 915 **Morbeck ME, Zihlman AL** (1988) Body composition and limb proportions. In:
916 Schwartz JH editor. *Orangutan biology*. Oxford: Oxford University Press. 285-297.
- 917 **Myatt JP, Crompton RH, Thorpe SKS** (2011) Hindlimb muscle architecture in
918 non-human great apes and a comparison of methods for analysing inter-species
919 variation. *Journal of Anatomy* **219** (2), 150-166.
- 920 **Myers CA, Register BC, Lertwanich P, et al.** (2011) Role of the Acetabular Labrum
921 and the Iliofemoral Ligament in Hip Stability: An in vitro Biplane Fluoroscopy Study.
922 *The American Journal of Sports Medicine* **39** (1), 85-91.
- 923 **Nakano Y, Hirasaki E, Kumakura H** (2006) Patterns of Vertical Climbing in Primates.
924 In: Ishida H Tuttle R Pickford M Ogihara N Nakatsukasa M (eds). *Human Origins and*
925 *Environmental Backgrounds Developments in Primatology: Progress and Prospects*.
926 Springer Boston, MA.
- 927 **Novacheck TF** (1998) The biomechanics of running. *Gait and Posture* **7**, 77-95.
- 928 **Odgaard A** (1997) Three-dimensional methods for quantification of cancellous bone
929 architecture. *Bone* **20** (4), 315-328.
- 930 **O'Neill MC, Lee L, Demes B, et al.** (2015) Three-dimensional kinematics of the
931 pelvis and hind limbs in chimpanzee (*Pan troglodytes*) and human bipedal walking.
932 *Journal of Human Evolution* **86**, 32-42.
- 933 **Ounpuu S** (1990) The biomechanics of running: a kinematic and kinetic analysis.
934 *AAOS Instructional Course Lectures* **39**, 305-318.
- 935 **Ounpuu S** (1994) The biomechanics of walking and running. *Clinics in Sports*
936 *Medicine* **13** (4), 843-863.
- 937 **Paul JP** (1976) Approaches to design- Force actions transmitted by joints in the
938 human body. *Proceedings of the Royal Society of London B* **192**, 163-172.
- 939 **Payne RC, Crompton RH, Isler K, et al.** (2006) Morphological analysis of the
940 hindlimb in apes and humans II Moment arms. *Journal of anatomy* **208** (6), 725-742.
- 941 **Pearson OM, Lieberman DE** (2004) The aging of Wolff's law: Ontogeny and
942 responses to mechanical loading in cortical bone. *American Journal of Physical*
943 *Anthropology* **125** (39), 63-99.
- 944 **Pedersen DR, Brand RA, Davy DT** (1997) Pelvic muscle and acetabular contact
945 forces during gait. *Journal of biomechanics* **30** (9), 959-965.

- 946 **Polk JD, Blumenfeld J, Ahlumwalia D** (2008) Knee posture predicted subchondral
947 apparent density in the distal femur: an experimental validation. *Anatomical Record*
948 **291**, 293-302.
- 949 **Pontzer H, Lieberman DE, Momin E, et al.** (2006) Trabecular bone in the bird knee
950 responds with high sensitivity to changes in load orientation. *Journal of Experimental*
951 *Biology* **209** (1), 57-65.
- 952 **R Development Core Team** (2017) R: A language and environment for statistical
953 computing. Vienna, Austria: The R Foundation for Statistical Computing.
- 954 **Rafferty KL, Ruff CB** (1994) Articular structure and function in *Hylobates Colobus*
955 and *Papio*. *American Journal of Physical Anthropology* **94** (3), 395-408.
- 956 **Rafferty KL** (1998) Structural design of the femoral neck in primates. *Journal of*
957 *Human Evolution* **34** (4), 361-383.
- 958 **Raichlen DA, Gordon AD, Harcourt-Smith WEH, et al.** (2010) Laetoli Footprints
959 Preserve Earliest Direct Evidence of Human-Like Bipedal Biomechanics. *PLOS ONE* **5**
960 (3), e9769.
- 961 **Reissis D, Abel RL** (2012) Development of fetal trabecular micro-architecture in the
962 humerus and femur. *Journal of anatomy* **220** (5), 496-503.
- 963 **Remis MJ** (1995) Effects of body size and social context on the arboreal activities of
964 lowland gorillas in the Central African Republic. *American Journal of Physical*
965 *Anthropology* **97** (4), 413-433.
- 966 **Remis MJ** (1999) Tree structure and sex differences in arboreality among western
967 lowland gorillas (*Gorilla gorilla gorilla*) at Bai Hokou Central African Republic.
968 *Primates* **40** (2), 383.
- 969 **Rodan GA** (1998) Bone homeostasis. *Proceedings of the National Academy of*
970 *Sciences* **95** (23), 13361-13362.
- 971 **Rubin CT, Turner AS, Bain S, et al.** (2001) Low mechanical signals strengthen long
972 bones. *Nature* **412**, 603.
- 973 **Rubin CT, McLeod KJ, Bain SD** (1990) Functional strains and cortical bone
974 adaptation: Epigenetic assurance of skeletal integrity. *Journal of Biomechanics* **23**, 43-
975 49.
- 976 **Ruff CB, Scott WW, Liu AY-C** (1991) Articular and diaphyseal remodeling of the
977 proximal femur with changes in body mass in adults. *American Journal of Physical*
978 *Anthropology* **86**, 397-413.
- 979 **Ruff CB, Higgins R** (2013) Femoral neck structure and function in early hominins.
980 *American Journal of Physical Anthropology* **150** (4) 512-525.
- 981 **Ruff CB, Runestad JA** (1992) Primate limb bone structural adaptations. *Annual*
982 *Review of Anthropology* **21**, 407-433.
- 983 **Ruff CB** (1995) Biomechanics of the hip and birth in early Homo. *American Journal of*
984 *Physical Anthropology* **98** (4), 527-574.

- 985 **Ruff CB** (2002) Long bone articular and diaphyseal structure in old world monkeys
986 and apes I: Locomotor effects. *American Journal of Physical Anthropology* **119** (4),
987 305-342.
- 988 **Ryan TM, Carlson KJ, Gordon AD, Jablonski N, Shaw CN, Stock JT** (2018) Hyman-
989 like hip joint loading in *Australopithecus africanus* and *Paranthropus robustus*. *Journal*
990 *of Human Evolution* **121**, 12-24.
- 991 **Ryan TM, Ketcham RA** (2002) The three-dimensional structure of trabecular bone in
992 the femoral head of strepsirrhine primates. *Journal of human evolution* **43** (1), 1-26.
- 993 **Ryan TM, Ketcham RA** (2005) Angular orientation of trabecular bone in the femoral
994 head and its relationship to hip joint loads in leaping primates. *Journal of Morphology*
995 **265** (3), 249-263.
- 996 **Ryan TM, Krovitz GE** (2006) Trabecular bone ontogeny in the human proximal
997 femur. *Journal of Human Evolution* **51** (6), 591-602.
- 998 **Ryan TM, Shaw CN** (2012) Unique Suites of Trabecular Bone Features Characterize
999 Locomotor Behavior in Human and Non-Human Anthropoid Primates. *PLOS ONE* **7**
1000 (7), e41037.
- 1001 **Ryan TM, Shaw CN** (2013) Trabecular bone microstructure scales allometrically in
1002 the primate humerus and femur. *Proceedings of the Royal Society B: Biological*
1003 *Sciences* **280** (1758), 20130172.
- 1004 **Ryan TM, Shaw CN** (2015) Gracility of the modern *Homo sapiens* skeleton is the
1005 result of decreased biomechanical loading. *Proceedings of the National Academy of*
1006 *Sciences* **112** (2), 372-377
- 1007 **Ryan TM, Walker A** (2010) Trabecular Bone Structure in the Humeral and Femoral
1008 Heads of Anthropoid Primates. *The Anatomical Record: Advances in Integrative*
1009 *Anatomy and Evolutionary Biology* **293** (4), 719-729.
- 1010 **Saers JPP, Cazorla-Bak Y, Shaw CN, et al.** (2016) Trabecular bone structural
1011 variation throughout the human lower limb. *Journal of Human Evolution* **97**, 97-108.
- 1012 **San Millán M, Kaliontzopoulou A, Rissech C, et al.** (2015) A geometric
1013 morphometric analysis of acetabular shape of the primate hip joint in relation to
1014 locomotor behaviour. *Journal of Human Evolution* **83**, 15-27.
- 1015 **Scherf H, Tilgner R** (2009) A new high-resolution computed tomography (CT)
1016 segmentation method for trabecular bone architectural analysis. *American Journal of*
1017 *Physical Anthropology* **140** (1), 39-51.
- 1018 **Scherf H** (2008) Locomotion-related Femoral Trabecular Architectures in Primates —
1019 High Resolution Computed Tomographies and Their Implications for Estimations of
1020 Locomotor Preferences of Fossil Primates. in Endo H, Frey R (eds). *Anatomical*
1021 *Imaging: Towards a New Morphology*. Springer Japan, Tokyo. 39-59.
- 1022 **Scherf H, Harvati K, Hublin J-J** (2013) A comparison of proximal humeral cancellous
1023 bone of great apes and humans *Journal of Human Evolution* **65** (1), 29-38.

- 1024 **Schneider CA, Rasband WS, Eliceiri KW** (2012) NIH Image to ImageJ: 25 years of
1025 Image Analysis. *Nature methods* **9** (7), 671-675.
- 1026 **Schultz AH** (1969) Observations on the Acetabulum of Primates. *Folia Primatologica*
1027 **11** (3), 181-199.
- 1028 **Shaw CN, Ryan TM** (2012) Does skeletal anatomy reflect adaptation to locomotor
1029 patterns? cortical and trabecular architecture in human and nonhuman anthropoids.
1030 *American Journal of Physical Anthropology* **147** (2), 187-200.
- 1031 **Simkin A, Ayalon J, Leichter I** (1987) Increased trabecular bone density due to
1032 bone-loading exercises in postmenopausal osteoporotic women. *Calcified tissue*
1033 *international* **40** (2), 59-63.
- 1034 **Skinner MM, Stephens NB, Tsegai ZJ, et al.** (2015) Human-like hand use in
1035 *Australopithecus africanus*. *Science* **347** (6220), 395-399.
- 1036 **Slocum DB, James SL** (1968) Biomechanics of Running. *JAMA* **205** (11), 721-728.
- 1037 **Smith DM, Nance WE, Kang KW, et al.** (1973) Genetic Factors in Determining Bone
1038 Mass. *The Journal of clinical investigation* **52** (11), 2800-2808.
- 1039 **Sonntag CF** (1923) On the Anatomy Physiology and Pathology of the Chimpanzee.
1040 *Proceedings of the Zoological Society of London* **93** (2), 323-429.
- 1041 **Sonntag CF** (1924) 17 On the Anatomy Physiology and Pathology of the Orang-
1042 Outan. *Proceedings of the Zoological Society of London* **94** (2), 349-450.
- 1043 **Stephens NB, Kivell TL, Thomas G, et al.** (2016) Trabecular architecture in the
1044 thumb of *Pan* and *Homo*: implications for investigating hand use loading and hand
1045 preference in the fossil record. *American Journal of Physical Anthropology* **161** (4),
1046 603-619.
- 1047 **Stern Jr JT, Susman RL** (1983) The locomotor anatomy of *Australopithecus*
1048 *afarensis*. *American Journal of Physical Anthropology* **60** (3), 279-317.
- 1049 **Sugardjito J, van Hooff JARAM** (1986) Age-Sex Class Differences in the Positional
1050 Behaviour of the Sumatran Orang-Utan (*Pongo pygmaeus abelii*) in the Gunung
1051 Leuser National Park Indonesia. *Folia Primatologica* **47** (1), 14-25.
- 1052 **Susman RL, Stern J JT, Jungers WL** (1984) Arboreality and Bipedality in the Hadar
1053 Hominids *Folia Primatologica* **43** (2-3), 113-156.
- 1054 **Suuriniemi M, Anitta M, Vuokko K, et al.** (2004) Association Between Exercise and
1055 Pubertal BMD Is Modulated by Estrogen Receptor α Genotype. *Journal of Bone and*
1056 *Mineral Research* **19** (11), 1758-1765.
- 1057 **Suwa G, Lovejoy CO, Asfaw B, et al.** (2012) Proximal Femoral Musculoskeletal
1058 Morphology of Chimpanzees and its Evolutionary Significance: A Critique of
1059 Morimoto et al (2011). *The Anatomical Record: Advances in Integrative Anatomy and*
1060 *Evolutionary Biology* **295** (12), 2039-2044

- 1061 **Sylvester AD, Terhune CE** (2017) Trabecular mapping: Leveraging geometric
1062 morphometrics for analyses of trabecular structure. *American Journal of Physical*
1063 *Anthropology* **163** (3), 553-569.
- 1064 **Thomason JJ** (1985a) Estimation of locomotory forces and stresses in the limb bones
1065 of Recent and extinct equids. *Paleobiology* **11** (2), 209-220.
- 1066 **Thomason JJ** (1985b) The Relationship of Trabecular Architecture to Inferred
1067 Loading Patterns in the Third Metacarpals of the Extinct Equids *Merychippus* and
1068 *Mesohippus*. *Paleobiology* **11** (3), 323-335.
- 1069 **Thorpe SKS, Crompton RH** (2005) Locomotor ecology of wild orangutans (*Pongo*
1070 *pygmaeus abelii*) in the Gunung Leuser Ecosystem Sumatra Indonesia: A multivariate
1071 analysis using log-linear modelling. *American Journal of Physical Anthropology* **127**
1072 (1), 58-78.
- 1073 **Thorpe SKS, Crompton RH** (2006) Orangutan positional behavior and the nature of
1074 arboreal locomotion in Hominoidea. *American Journal of Physical Anthropology* **131**
1075 (3), 384-401.
- 1076 **Thorpe SKS, Holder R, Crompton RH** (2008) Orangutans employ unique strategies
1077 to control branch flexibility. *Proceedings of the National Academy of Sciences of the*
1078 *United States of America* **106** (31), 12646-12651.
- 1079 **Treese GM, Gee AH** (2014) Independent measurement of femoral cortical thickness
1080 and cortical bone density using clinical CT. *Medical Image Analysis* **20** (1), 249-264.
- 1081 **Tsegai ZJ, Kivell TL, Gross T, et al.** (2013) Trabecular Bone Structure Correlates with
1082 Hand Posture and Use in Hominoids. *PLOS ONE* **8** (11), e78781.
- 1083 **Tsegai ZJ, Skinner MM, Gee AH, et al.** (2017) Trabecular and cortical bone
1084 structure of the talus and distal tibia in *Pan* and *Homo*. *American Journal of Physical*
1085 *Anthropology* **163**, 784-805.
- 1086 **Tsegai ZJ, Skinner MM, Pahr DH, et al.** (2018) Systemic patterns of trabecular bone
1087 across the human and chimpanzee skeleton. *Journal of anatomy* **232** (4), 641-656.
- 1088 **Tuttle RH, Cortright W** (1988) Positional behavior adaptive complexes and
1089 evolution. In: Schwartz JH editor. *Orangutan biology*. Oxford: Oxford University Press.
1090 311-330.
- 1091 **Van der Bogert AJ, Read L, Nigg BM** (1999) An analysis of hip joint loading during
1092 walking running and skiing. *Medicine, Science in Sports, Exercise* **31** (1), 131-142.
- 1093 **Volpato V, Viola TB, Nakatsukasa M, et al.** (2008) Textural characteristics of the
1094 iliac-femoral trabecular pattern in a bipedally trained Japanese macaque. *Primates* **49**
1095 (1), 16-25.
- 1096 **Wagner FV, Negrão JR, Campos J, et al.** (2012) Capsular Ligaments of the Hip:
1097 Anatomic Histologic and Positional Study in Cadaveric Specimens with MR
1098 Arthrography. *Radiology* **263** (1), 189-198.

- 1099 **Wallace IJ, Demes B, Judex S** (2017) Ontogenetic and Genetic Influences on Bone's
1100 Responsiveness to Mechanical Signals. In Percival CJ, Richtsmeier JT (eds). *Building*
1101 *Bones: Bone Formation and Development in Anthropology*. Cambridge University
1102 Press, Cambridge. 233-253
- 1103 **Wallace IJ, Demes B, Mongle C, et al.** (2014) Exercise-Induced Bone Formation Is
1104 Poorly Linked to Local Strain Magnitude in the Sheep Tibia. *PLOS ONE* **9** (6), e99108.
- 1105 **Walsh JS** (2015) Normal bone physiology remodelling and its hormonal regulation.
1106 *Surgery (Oxford)* **33** (1), 1-6.
- 1107 **Ward CV** (1991) Functional anatomy of the lower back and pelvis of the Miocene
1108 hominoid *Proconsul nyanzae* from Mfanga Island Kenya. PhD Dissertation Johns
1109 Hopkins University.
- 1110 **Ward CV** (2002) Interpreting the posture and locomotion of *Australopithecus*
1111 *afarensis*: Where do we stand? *American Journal of Physical Anthropology* **119** (35),
1112 185-215.
- 1113 **Ward FO** (1838) *Outlines of Human Osteology*. London: Henry Renshaw.
- 1114 **Whalen RT, Carter DR, Steele CR** (1988) Influence of physical activity on the
1115 regulation of bone density. *Journal of Biomechanics* **21** (10), 825-837.
- 1116 **Whitehouse WJ** (1974) The quantitative morphology of anisotropic trabecular bone.
1117 *Journal of microscopy* **101** (2), 153-168.
- 1118 **Wolff J** (1892) *Das Gesetz der Transformation der Knochen*. Berlin: A Hirchwild.
- 1119 **Wolff J** (1986) *The law of bone remodeling*. Berlin: Springer-Verlag.
- 1120 **Yoshida H, Faust A, Wilckens J, et al.** (2006) Three-dimensional dynamic hip
1121 contact area and pressure distribution during activities of daily living. *Journal of*
1122 *Biomechanics* **39** (11), 1996-2004.

1123
1124
1125
1126
1127
1128
1129
1130
1131
1132
1133
1134
1135
1136
1137
1138
1139
1140
1141
1142
1143
1144
1145
1146
1147
1148
1149
1150
1151
1152
1153
1154
1155
1156
1157
1158
1159
1160
1161
1162
1163
1164
1165

For Peer Review Only

1166

1167

1168

1169 **Tables**

1170

1171 **Table 1. Study sample taxonomic composition, re-sampled voxel size range,**
 1172 **sex, and microCT scanning parameters. All specimens were re-sampled except six**
 1173 **of the gorillas that were scanned at lower resolutions.**

Taxon	Locomotor mode	N	Sex	Voxel size (mm)	Scanning
<i>Pan troglodytes</i>	Arboreal/ knuckle-walker	20	13 female, 6 male, 1 unknown	0.04-0.05	kV:120-130, μ A: 80- 100, 0.25 or 0.5mm brass
<i>Gorilla gorilla gorilla</i>	Terrestrial knuckle-walker	14	7 female, 7 male	0.05-0.08	kV:130-170, μ A: 110- 160, 0.1-0.5mm copper
<i>Pongo sp.</i>	Arboreal/ torso- orthograde suspension	5	5 female	0.04-0.045	kV:140, μ A: 140, 0.5mm brass
<i>Homo sapiens</i>	Bipedal	12	3 female, 8 male, 1 unknown	0.06-0.07	kV:130-140, μ A: 100- 140, 0.5mm brass

1174

1175

1176

1177

1178

1179

1180

1181

1182

1183

1184

1185

1186

1187

1188

1189

1190

1191
1192
1193
1194
1195
1196
1197

1198 **Table 2. Trabecular architecture results.** Mean, standard deviation (in parentheses)
1199 and coefficient of variation for five trabecular parameters quantified throughout the
1200 femoral head.

Taxon	<i>Pan</i>	CV	<i>Gorilla</i>	CV	<i>Pongo</i>	CV	<i>Homo</i>	CV
BV/TV	0.39 (0.03)	8.6	0.35 (0.05)	14.8	0.33 (0.04)	13.4	0.30 (0.05)	16.0
DA	0.15 (0.03)	21.6	0.18 (0.04)	21.8	0.15 (0.02)	14.7	0.23 (0.04)	17.9
Tb.N (1/mm)	1.19 (0.11)	9.4	0.83 (0.09)	10.7	0.92 (0.04)	4.4	0.87 (0.1)	11.4
Tb.Sp (mm)	0.56 (0.06)	10.0	0.81 (0.08)	9.8	0.78 (0.07)	8.4	0.84 (0.14)	16.6
Tb.Th (mm)	0.29 (0.03)	11.8	0.40 (0.08)	19.1	0.31 (0.03)	10.9	0.32 (0.03)	9.9

1201
1202
1203
1204
1205
1206
1207
1208
1209
1210
1211
1212
1213
1214
1215
1216
1217

1218
1219
1220
1221
1222
1223
1224
1225
1226
1227
1228
1229
1230

1231 **Table 3. Results of pairwise comparisons between taxa.** Bonferroni-corrected p-
1232 values of each pairwise comparison for all trabecular parameters. Significant results
1233 are indicated by grey shading.

	<i>Pan-Gorilla</i>	<i>Pan - Pongo</i>	<i>Pan - Homo</i>	<i>Gorilla - Pongo</i>	<i>Gorilla - Homo</i>	<i>Pongo - Homo</i>
BV/TV	0.14	<0.05	<0.001	1	0.14	1
DA	0.24	1	<0.001	1	<0.05	<0.01
Tb.N	<0.001	<0.01	<0.001	0.33	1	1
Tb.Sp	<0.001	<0.001	<0.001	1	1	1
Tb.Th	<0.001	1	<0.05	0.09	0.05	1

1234
1235
1236
1237
1238
1239
1240
1241
1242
1243
1244
1245
1246
1247
1248
1249
1250

1251
1252
1253
1254
1255
1256
1257
1258
1259
1260
1261
1262
1263
1264
1265
1266
1267
1268
1269

1270 **Figure legends**

1271
1272
1273
1274
1275
1276
1277
1278

Figure 1. Comparison of hip posture during different habitual locomotor activities in great apes (A-B) and humans (C-D). (A) Great ape hip posture in maximum hip flexion (~55-60 degrees) during climbing (Isler, 2005). (B) Great ape hip posture at toe-off (~110 degrees) during terrestrial knuckle-walking (Finestone et al. 2018). (C) Human hip posture at toe-off (~175 degrees). (D) Human hip posture at heel-strike (~160 degrees).

1279
1280
1281
1282
1283
1284

Figure 2. *Pan* BV/TV distribution in the femoral head. Five *Pan* specimens showing variation in the BV/TV distribution across the sample in (A) anterior, (B) posterior and (C) superior views. BV/TV is scaled to 0-0.55. All specimens are from the right side. Specimens from left to right (F-female, M-male): MPITC 14996 (F), USNM 220063 (F), USNM 176228 (M), MPITC 11781 (M), MPITC 11786 (F).

1285
1286
1287
1288
1289
1290

Figure 3. *Gorilla* BV/TV distribution in the femoral head. Five *Gorilla* specimens showing variation in the BV/TV distribution across the sample in (A) anterior, (B) posterior and (C) superior views. BV/TV is scaled to 0-0.55. All specimens are from the right side. Specimens from left to right (F-female, M-male): M96 (F), M264 (M), M372 (M), M856 (F), FC123 (M).

1291
1292
1293

Figure 4. *Pongo* BVTV distribution in the femoral head. Five *Pongo* specimens showing variation in the BV/TV distribution across the sample in (A) anterior, (B) posterior and (C) superior views. BV/TV is scaled to 0-0.55. All specimens are from

1294 the right side. Specimens from left to right (All female): ZSM 1909 0801, 1907 0660,
1295 1973 0270, 1907 0483, 1907 0633b.

1296

1297 **Figure 5. *Homo* BV/TV distribution in the femoral head.** Five *Homo* specimens
1298 showing variation in the BV/TV distribution across the sample in (A) anterior, (B)
1299 posterior and (C) superior views. BV/TV is scaled to 0-0.55. All specimens are from
1300 the right side. Specimens from left to right (F-female, M-male): CAMPUS 36 (F),
1301 CAMPUS 93 (M), CAMPUS 74 (F), CAMPUS 417 (sex unknown), CAMPUS 81 (M).

1302

1303 **Figure 6. Bivariate plot of mean bone volume fraction (BV/TV) and mean**
1304 **degree of anisotropy (DA) for each individual and species in the sample.**

1305

1306 **Figure 7. A histogram of mean BV/TV and DA value distributions in the studied**
1307 **taxa.**